Carbohydrate Polymers 83 (2011) 1766–1774

Contents lists available at ScienceDirect

Carbohydrate Polymers

journal homepage: www.elsevier.com/locate/carbpol

# Aerocellulose from cellulose–ionic liquid solutions: Preparation, properties and comparison with cellulose–NaOH and cellulose–NMMO routes

Romain Sescousse, Roxane Gavillon [1], Tatiana Budtova *

*Mines ParisTech, Centre de Mise en Forme des Matèriaux - CEMEF[2], UMR CNRS/Ecole des Mines de Paris 7635, BP 207, 06904 Sophia-Antipolis, France*

ARTICLE INFO

*Article history:*
Received 31 August 2010
Received in revised form 8 October 2010
Accepted 19 October 2010
Available online 27 October 2010

*Keywords:*
Cellulose
Imidazolium-based ionic liquids
Regeneration kinetics
Diffusion
Cellulose–NaOH–water solution
Mechanical properties
Porosity
Morphology
Aerogel

ABSTRACT

Ultra-light and highly porous cellulose material, aerocellulose, is prepared via cellulose dissolution in imidazolium-based ionic liquids, 1-ethyl-3-methylimidazolium acetate (EMIMAc) and 1-butyl-3-methylimidazolium chloride (BMIMCl), followed by regeneration and drying in supercritical $CO_2$ conditions. Regeneration kinetics of cellulose in water is studied. The diffusion coefficients of EMIMAc and BMIMCl were obtained using a Fickian approach; they are analysed as a function of cellulose concentration and compared with the previously obtained values for NaOH and *N*-methyl-morpholine *N*-oxide (NMMO). Density, morphology and porosity of aerocellulose from cellulose–ionic liquid solutions are investigated and compared with the corresponding values from NaOH and NMMO routes. The mechanical properties of aerocelluloses under compression from all three routes are studied and correlated with the moduli obtained from mercury porosimetry. For the ionic liquid and NaOH routes the Young's modulus scales aerocellulose density with the exponent close to three, a value typical for silica aerogels.



## 1. Introduction

The use of cellulose, an inexhaustible natural polymer, is reconsidered in our days due to the discoveries of new non-toxic cellulose solvents and the possibilities of making materials with various functionalities. Ultra-light and highly porous cellulose is a new very promising material offering a wide range of potential applications, from bio-medical and cosmetics (delivery systems, scaffolds) to insulation and electro-chemical (when pyrolysed).

Two main ways of making ultra-light cellulose are known. One is inspired by the preparation of aerogels. Cellulose is dissolved in a direct solvent (such as *N*-methyl-morpholine *N*-oxide (NMMO) monohydrate (Innerlohinger, Weber, & Kraft, 2006; Liebner, Potthast, Rosenau, Haimer, & Wendland, 2008), 8% NaOH–water (Gavillon & Budtova, 2008; Sescousse & Budtova, 2009), LiCl/DMAc (Duchemin, Staiger, Ticker, & Newman, 2010), calcium thiocyanate (Jin, Nishiyama, Wada, & Kuga, 2004) or ionic liquid (Aaltonen & Jauhiainen, 2009; Deng, Zhou, Du, Kasteren, & Wang, 2009; Tsioptsias, Stefopoulos, Kokkinomalis, Papapdoupoulou, & Panayiotou, 2008), regenerated (or coagulated) in a non-solvent (water, alcohols) and then dried in a special way that prevents pores collapse, i.e. either via freeze-drying (Deng et al., 2009; Duchemin et al., 2010; Jin et al., 2004), or under $CO_2$ supercritical conditions (Aaltonen & Jauhiainen, 2009; Gavillon & Budtova, 2008; Innerlohinger et al., 2006; Liebner et al., 2008; Sescousse & Budtova, 2009; Tsioptsias et al., 2008). In all cases cited no chemical cross-linking is used to "stabilize" the cellulose "network"; it is formed during cellulose regeneration either from a solution (Aaltonen & Jauhiainen, 2009; Deng et al., 2009; Duchemin et al., 2010; Innerlohinger et al., 2006; Jin et al., 2004; Liebner et al., 2008) or from a physical gel (Gavillon & Budtova, 2008; Sescousse & Budtova, 2009). These cellulose II aerogel-like materials, referred to as aerocellulose (Duchemin et al., 2010; Gavillon & Budtova, 2008; Innerlohinger et al., 2006; Sescousse & Budtova, 2009), have wide pore size distribution, from tens of nanometers to several microns, and a high specific surface area of several hundreds of $m^2/g$. The density of aerocellulose depends on the initial cellulose concentration in solution and on the control of drying. Foaming agents can be added to increase aerocellulose porosity (Gavillon & Budtova, 2008).

The second way of making ultra-light porous cellulose is to use cellulose nanofibers, which can be either bacterial cellulose

* Corresponding author. Tel.: +33 4 93 95 74 70; fax: +33 4 92 38 97 52.
*E-mail address:* Tatiana.Budtova@mines-paristech.fr (T. Budtova).
[1] Present address: L'Oreal, 188-200, rue Paul Hochart, 94550 Chevilly-Larue, France.
[2] Member of the European Polysaccharide Network of Excellence (EPNOE), www.epnoe.eu.

0144-8617/$ – see front matter © 2010 Elsevier Ltd. All rights reserved.
doi:10.1016/j.carbpol.2010.10.043

(Liebner et al., 2010; Maeda, Nakajima, Hagwara, Sawaguchi, & Yano, 2006) or microfibrillated cellulose prepared via native cellulose mechanical disintegration and enzymatic treatment (Paakko et al., 2008). In both cases the starting material is a network of cellulose I nanofibers filled with water. Water can then be extracted using the same approaches as described for aerocellulose, i.e. freeze-drying or drying in supercritical $CO_2$. The resulting material is thus also a network of cellulose I nanofibers. It looks similar to aerocellulose but with higher porosities and lower densities because of lower initial cellulose concentrations and absence of contraction during drying due to higher skeleton crystallinity and molecular weight. However, the preparation of porous cellulose from the nanofiber route either does not allow the variation of cellulose concentrations (case of bacterial cellulose), or requires high energy consumption (in the case of microfibrillated cellulose).

In general, aerocellulose can be prepared from any cellulose solution. Many cellulose solvents are known, but most are either toxic, or with some drawback effects or, like (7–9%) NaOH–water–urea (or thiourea) mixtures, do not allow the dissolution of cellulose of high molecular weights and concentrations (Egal, Budtova, & Navard, 2007). Room-temperature imidazolium-based ionic liquids (IL), such as 1-ethyl-3-methylimidazolium acetate (EMIMAc), 1-butyl-3-methylimidazolium chloride (BMIMCl) and 1-allyl-3-methylimidazolium chloride, are now accepted to be direct cellulose solvents (Swatloski, Spear, Holbrey, & Rogers, 2002; Zhang, Wu, Zhang, & He, 2005). Processing of cellulose from ionic liquids, which occurs without a derivatisation step, is very attractive: the dissolution procedure is simple and ionic liquids are nonvolatile and have a high thermal stability making them so called "green solvents". Cellulose of high molecular weight and at rather high concentrations, around 15–20%, can be dissolved in the above mentioned ionic liquids. Various cellulose objects such as fibers (Cai, Zhang, Guo, Shao, & Hu, 2010; Quan, Kang, & Chin, 2010; Wendler, Kosan, Kreig, & Meister, 2009), films (Turner, Spear, Holbrey, & Rogers, 2004), composites (Zhao et al., 2009) and beads (Lin, Zhan, Liu, Fu, & Lucia, 2009) were prepared from cellulose–ionic liquid solutions.

In this work we present an extensive study of the preparation and properties of new aerocellulose prepared from cellulose–EMIMAc and cellulose–BMIMCl solutions, via dissolution/regeneration route and drying under supercritical $CO_2$. Carbon dioxide is one of the most commonly used supercritical fluids in polymer chemistry and technology due to its low cost, non-inflammability and low critical point temperature and pressure. Literature reports the preparation conditions and final morphology/porosity of aerocellulose prepared from either BMIMCl (Aaltonen & Jauhiainen, 2009; Deng et al., 2009) or AMIMCl (Tsioptsias et al., 2008). We start with a study of cellulose regeneration kinetics from ionic liquid solutions. To the best of our knowledge there is no publication describing this unavoidable step in cellulose processing from ionic liquids, whatever is the final material. Regeneration kinetics from ionic liquids is characterized by EMIMAc and BMIMCl diffusion into regenerating bath (in our case, water); the results obtained are compared with the ones known for cellulose regeneration from cellulose–NMMO monohydrate and cellulose NaOH–water systems (Gavillon & Budtova, 2007). Then we discuss aerocellulose density, porosity and morphology from cellulose–EMIMAc and again compare with the same from NMMO and NaOH routes. Finally, a systematic study of the mechanical properties of aerocelluloses made from EMIMAc, NMMO monohydrate and 8% NaOH–water were performed. The approaches developed for aerogels and foams were applied to analyse aerocellulose mechanical properties. Young modulus, compressive yield strength and absorption energy were obtained and studied as a function of aerocellulose density and preparation route.

## 2. Experimental

### 2.1. Materials

Avicel PH-101 microcrystalline cellulose ("cellulose" in the following) with degree of polymerization DP = 180, was purchased from Sigma–Aldrich and used for most of the studies (ionic liquid and NaOH routes). Other celluloses, Solucell from Lenzing AG, Austria, of DP = 950 (Solucell in the following) and cotton also of DP = 950 were used for NMMO route.

The ionic liquids EMIMAc and BMIMCl were used as received from Fluka. NaOH in pellets (97% purity) and acetone (98% purity) were purchased from VWR. Alkyl polyglycoside surfactant Simulsol SL8 was from Seppic Inc., Fairfield, USA. Distilled water was used for preparing cellulose–NaOH–water solutions and for regenerating bath. $CO_2$ for drying in supercritical conditions was supplied by Air Liquide with a purity of 99.9%.

### 2.2. Methods

#### 2.2.1. Preparation of samples: cellulose solutions, samples for regeneration studies and making dry aerocellulose

Cellulose was dried at 50 °C in vacuum prior to use. Cellulose–8% NaOH–water solutions were prepared as described elsewhere (Egal et al., 2007; Gavillon & Budtova, 2008; Sescousse & Budtova, 2009). Briefly, an aqueous solution of 12 wt% NaOH was cooled down to −6 °C. Cellulose was swollen in distilled water and kept at 5 °C. 12% NaOH–water and swollen-in-water-cellulose were mixed at −6 °C with a stirring rate of 1000 rpm for 2 h in certain proportions to obtain various cellulose concentrations (wt%) in 8% NaOH–water. Solutions were stored at 5 °C to avoid aging.

Cellulose–IL solutions were prepared by mixing and stirring cellulose and solvent in a sealed reaction vessel at 80 °C for about 48 h to ensure complete dissolution. Cellulose solutions were stored at room temperature and protected against moisture absorption.

In order to study cellulose regeneration kinetics from cellulose–IL solutions and to use the Fickian approach which was proved to work well for cellulose–NaOH–water and cellulose–NMMO monohydrate solutions (Gavillon & Budtova, 2007; Sescousse & Budtova, 2009), the sample must have well defined dimensions. An infinite plane approximation was selected because of the ease of sample preparation (Gavillon & Budtova, 2007; Sescousse & Budtova, 2009). Within this approximation sample thickness must not be larger than 1/10 of its diameter in case the sample is a disk. A special cylindrical mould of 3 cm diameter and thickness $2l$ = 3 mm was constructed. The walls of the mould were made of a stainless steel grid with the holes of 50 μm × 50 μm. The solution was pored into the mould, closed with the cover made of the same grid and placed into regenerating bath. Because cellulose–EMIMAc and cellulose–BMIMCl solutions are of a rather high viscosity (see, for example, Gericke, Schlufter, Liebert, Heinze, & Budtova, 2009; Sescousse, Le, Ries, & Budtova, 2010), they were not leaking through the holes. This set-up allowed free solvent/non-solvent diffusion through the mould walls and kept sample size constant during regeneration.

To prepare dry aerocellulose samples from cellulose–8% NaOH–water and cellulose–IL, the procedure described in Gavillon and Budtova (2008), Sescousse and Budtova (2009) was used, i.e. drying in supercritical $CO_2$ conditions. For the cellulose–NaOH–water route, solution gelation was performed prior regeneration: the solutions were kept at 50 °C for 2 h (Roy, Budtova, & Navard, 2003). For cellulose–IL route, the same mould, as described above, was used. Solutions and gels were then placed in water regenerating bath which was regularly changed until all solvent is washed out (control of pH for NaOH route and refractive index for ionic liquids, see next section). The samples were then

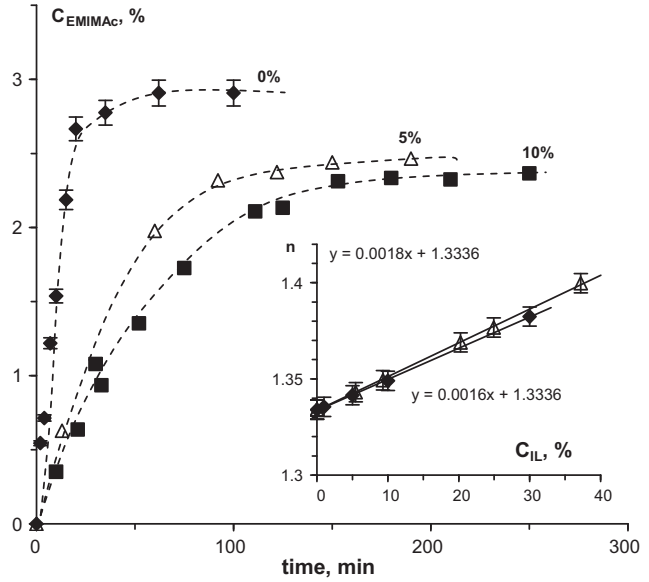


**Fig. 1.** Example of EMIMAc concentration increase in the regenerating bath in time during cellulose regeneration from cellulose–EMIMAc solutions at 22 °C. Cellulose initial concentrations shown are 0, 5 and 10%. Dashed lines are given to guide the eye. *Inset*: Calibration curves for EMIMAc (dark points) and BMIMCl (open points) aqueous solutions: refractive index vs IL concentration at 22 °C.

washed in acetone to remove water which is not compatible with $CO_2$. Swollen-in-acetone samples were dried under supercritical $CO_2$ as described earlier (1 L autoclave, 80 bar, 35 °C) (Gavillon & Budtova, 2008; Sescousse & Budtova, 2009). After depressurisation (4 bar per hour at 37 °C), aerocellulose samples were extracted and analysed.

In some cases of NaOH route, the surfactant Simulsol was used as a foaming agent to increase aerocellulose porosity, as described in Gavillon and Budtova (2008). Simulsol was added at various concentrations (0.1%, 0.5%, and 1% in weight) to the ready cellulose–8% NaOH–water solution. The mixture was stirred at 1000 rpm for 5 min at +5 °C, leading to the formation of air bubbles. The foamed solution was then immediately gelled at 50 °C for 2 h in order to "freeze" the bubbles. Simulsol dissolved in water during the regeneration step.

Aerocellulose prepared from Solucell and cotton dissolved in NMMO monohydrate was used to perform compression experiments to determine the mechanical properties and compare with NaOH and IL routes. The samples were prepared in the R&D laboratory of Lenzing AG, Austria. Solucell–NMMO monohydrate and cotton–NMMO monohydrate solutions were poured into cylindrical moulds, cooled down to room temperature and regenerated in water at ambient temperature. Water was exchanged with acetone of analytical grade. The samples were dried in $CO_2$ under supercritical conditions in Natex, Ternitz, Austria.

*2.2.2. Cellulose regeneration kinetics from ionic liquid solutions*

The kinetics of cellulose regeneration from solutions in ionic liquids was studied as follows. The mould with cellulose–IL solution of a given weight and volume was placed in the regenerating bath (water) of a fixed temperature. The proportion between sample/bath weights was about 1/30 with the bath volume of 100 mL. Magnetic stirrer with a gentle stirring rate (~300 rpm) was used for concentration homogenization.

The concentration of ionic liquid in water was measured using an Abbe refractometer. First, the calibration dependence was obtained by measuring the refractive index $n$ of IL–water solutions as a function of known IL concentration $C_{IL}$ (see inset of Fig. 1). Calibrations were carried out at each bath temperature. When cellulose was regenerating, small amounts of bath liquid were taken at different times. Because the concentrations of IL in regenerating bath were very low, it was not possible to use directly the calibration dependence. First, water from the probes was evaporated in a controlled way in order to increase IL concentration. Then the refractive index was measured and IL concentration in the bath was calculated with the help of the calibration dependence and knowing the weights of the probes before and after evaporation. These data were used to describe the kinetics of IL release from the sample (see example for cellulose regeneration from cellulose–EMIMAc solution in Fig. 1). Each experiment was repeated 3–5 times and the mean value of the diffusion coefficient was calculated as will be described in Section 3. The error in concentration determination is within 5% and for the resulting diffusion coefficient it was about 15%.

*2.2.3. Mechanical measurements*

Compression mechanical measurements were performed on dry aerocelluloses from IL, NaOH and NMMO routes. The samples were cylinders with the height being 1.5 times larger than the diameter.

The universal testing machine, Dartec Testwell was used for the uniaxial compression tests. The compressive machine was equipped with a 50 kN load cell. The cylindrical sample was inserted between two steel circular compression plates. A deformation rate of 0.0027 $s^{-1}$ was applied on the top surface of each specimen. All measurements were made under ambient conditions at about 20–22 °C and 50–60% relative humidity.

*2.2.4. Porosity measurements*

Porosity of aerocellulose was measured in SAFT, Bordeaux, France, using mercury intrusion with Micromeritics Autopore IV porosimeter and nitrogen absorption with Belsorp Mini II. The details on data treatment will be given in Section 3.

The density of all aerocelluloses was determined by measuring the weight and dimensions of the samples.

*2.2.5. Scanning electron microscopy*

Scanning electron microscopy (SEM) observations of aerocellulose morphology were performed using a PHILIPS XL30 ESEM at the acceleration voltage of 10–15 kV. Thin layers of gold were deposited by sputtering onto the surface of the cross sections.

## 3. Results and discussion

*3.1. Cellulose regeneration kinetics from cellulose–IL solutions*

As demonstrated in Sescousse and Budtova (2009), Gavillon and Budtova (2007), Biganska and Navard (2005), regeneration of cellulose from cellulose–NaOH–water and cellulose–NMMO monohydrate solutions is a diffusion-controlled process and can be described by a Fickian approach. The same is to be expected for the description of cellulose regeneration from cellulose–IL solutions: indeed, cumulated amount of solvent $M(t)$ released in time $t$ as a function of $\sqrt{t}$ is approximated with a straight line up to ≈80% of $M(t)$, which indicates a diffusion-controlled process.

The method used for the monitoring the amount of IL released into the bath in time allows determination of a mean value of diffusion coefficient which does not depend on the position inside the cellulose sample and is supposed to be constant. Several simplifications can be made for the calculation of IL diffusion coefficient; they are presented in Table 1. A relative mass of substance released in time $M(t)/M$ ($M$ being maximal amount of substance in the bath which corresponds to the mass of IL in cellulose sample) was plotted against $t/l^2$ ($l$ being half thickness of the sample disk) for each bath temperature and various cellulose concentration (see examples in Fig. 2). Diffusion coefficients of EMIMAc and BMIMCl were

**Table 1**
Approximations used to calculate the diffusion coefficient of a substance released from an infinite plane.

| | |
|---|---|
| Early time: $0 \leq \frac{M(t)}{M} \leq 0.4$ | $\frac{M(t)}{M} = 4\left(\frac{Dt}{\pi l^2}\right)^{1/2}$ |
| Half-time: $\frac{M(t)}{M} = 1/2$ | $D = \frac{0.049}{(t/l^2)_{atM(t)/M=0.5}}$ |
| Late-time: $0.4 \leq \frac{M(t)}{M} \leq 1$ | $\frac{M(t)}{M} = 1 - \frac{8}{\pi^2}\exp\left(\frac{-\pi^2 Dt}{l^2}\right)$ |

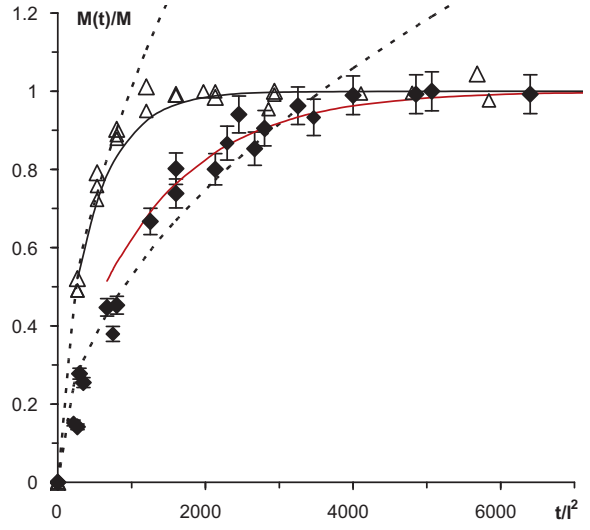


**Fig. 2.** Cumulated mass evolution of EMIMAc during regeneration of cellulose from 5% cellulose–EMIMAc solution at 22 °C (dark points) and at 54 °C (open points). Solid and dashed lines correspond to late time and early time approximations, respectively.

then calculated for each approximation and the average value was taken.

The diffusion coefficients of EMIMAc and BMIMCl at 22 °C are shown in Fig. 3 as a function of cellulose concentration. It was not possible to obtain $D_{BMIMCl}$ at $C_{cell}$ = 0% because of extremely high BMIMCl hygroscopicity and thus difficulties in sample preparation. The measured $D_{EMIMAc}$ in water at $C_{cell}$ = 0 was compared with $D_{EMIM^-}$ using data available in literature for the self-diffusion of $EMIM^-$ ions at 27 °C (Liu, Sale, Holmes, Simmons, & Singh, 2010)

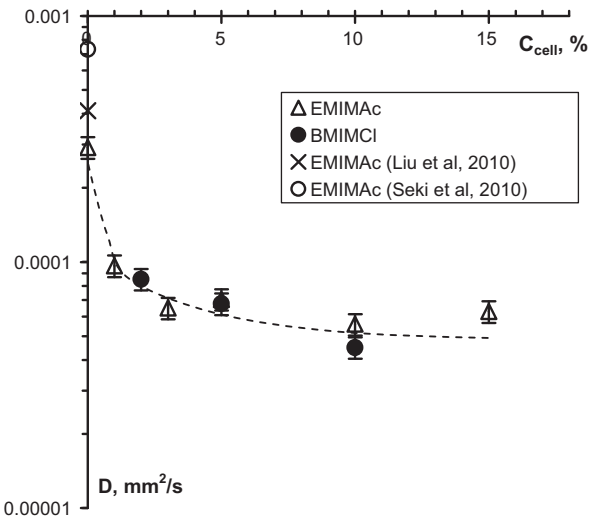


**Fig. 3.** . Diffusion coefficients of EMIMAc and BMIMCl as a function of cellulose concentration during cellulose regeneration in water at 22 °C. The line is given to guide the eye. $D_{EMIM^-}$ at $C_{cell}$ = 0 calculated using data from Liu et al. (2010) and Seki et al. (2010) are also shown.

and 30 °C (Seki et al., 2010). First, the radius $R$ of the ion was calculated using Einstein formula $D_{EMIM^-}(T) = k_B T/6\pi\eta(T)R$ where $k_B$ is Boltzmann constant, $T$ is temperature and $\eta$ is the viscosity of the medium (EMIMAc) which was taken from Gericke et al. (2009) at the corresponding temperatures, 27 °C and 30 °C. Then the radius obtained was used to calculate the diffusion coefficient of $EMIM^-$ in water taking water viscosity of $10^{-3}$ Pa s. For such a rough estimation, and also considering some difference in temperature (experimental vs used in literature), the agreement between measured and estimated EMIMAc diffusivity in water is very good, $3 \times 10^{-4}$ mm²/s (experimental value obtained in this work at 22 °C) vs $4 \times 10^{-4}$ at 27 °C calculated with self-diffusion data from Liu et al. (2010) and $7 \times 10^{-4}$ at 30 °C from Seki et al. (2010).

The values of $D_{EMIMAc}$ and $D_{BMIMCl}$ at the same cellulose concentration practically coincide within experimental error which was expected as far as both solvent are very similar. At a given cellulose concentration, $D_{EMIMAc}$ and $D_{BMIMCl}$ are four to five times lower than $D_{NaOH}$ (Gavillon & Budtova, 2007; Sescousse & Budtova, 2009) and about twice lower than $D_{NMMO}$ (Gavillon & Budtova, 2007) because of the larger size of the diffusing entity (ionic liquid). The presence of low amount of cellulose, 1%, strongly decreases IL diffusion coefficient as compared with $C_{cell}$ = 0. Further increase of cellulose concentration leads to a very small decrease in $D_{EMIMAc}$ and $D_{BMIMCl}$ (Fig. 3). Such a weak dependence of solvent diffusion coefficient on polymer concentration is rather unusual. The same trend was observed for $D_{NMMO}$ during cellulose regeneration while $D_{NaOH}$ was found to be concentration-dependent (Gavillon & Budtova, 2007). It was shown that free volume and hydrodynamic models seem to describe well the dependence of NaOH diffusion coefficient on cellulose concentration during regeneration, contrary to the case of cellulose–NMMO monohydrate system (Gavillon & Budtova, 2007). There are several reasons for this different concentration behaviour, $D_{NMMO}$ and $D_{IL}$ vs $D_{NaOH}$. First, cellulose–NMMO monohydrate or IL are real solutions and cellulose–NaOH is a gel which is formed due to the preferential cellulose–cellulose and not cellulose–solvent interactions at room temperature. The gelation of cellulose–NaOH–water solution with the increase of time and temperature is accompanied by a micro-phase separation. At the beginning of regeneration cellulose in 8% NaOH–water is already partly coagulated, it is a sort of a network where NaOH can freely diffuse, while NMMO or ionic liquid are diffusing in a polymer solution which is undergoing a phase separation when placed in a non-solvent. Second, the viscosity and composition of the medium where the solvent entity is diffusing varies a lot from the beginning to the end of cellulose regeneration for NMMO and ionic liquid system while it does not vary that much for NaOH system. For example, at the beginning of regeneration, in a 3% cellulose sample there is 97% of ionic liquid, 82% of NMMO and only 8% of NaOH. At the end of the experiment the concentration of IL, NMMO and NaOH is theoretically zero. There is thus a strong gradient of IL and NMMO concentration in the regenerating cellulose. Thus the average diffusion approach used here cannot be applied for interpreting the dependence of ionic liquid and NMMO diffusion coefficients on cellulose concentration.

The diffusion coefficients of EMIMAc and BMIMCl at various bath temperatures were measured for 5% cellulose solutions. As expected, the higher bath temperature, the quicker the cellulose regeneration (see example in Fig. 2). The activation energy was calculated from the temperature dependence of EMIMAc and BMIMCl diffusion coefficients. It was found to be 15–20 kJ/mol which is comparable with the values of the activation energies obtained for NaOH and NMMO diffusion coefficients at this cellulose concentration (Gavillon & Budtova, 2007). Overall, the kinetics of cellulose regeneration from cellulose–EMIMAc and cellulose–BMIMCl solutions is very similar. Knowing the diffusion coefficient at a given temperature, it is then easy to estimate the time needed to regen-

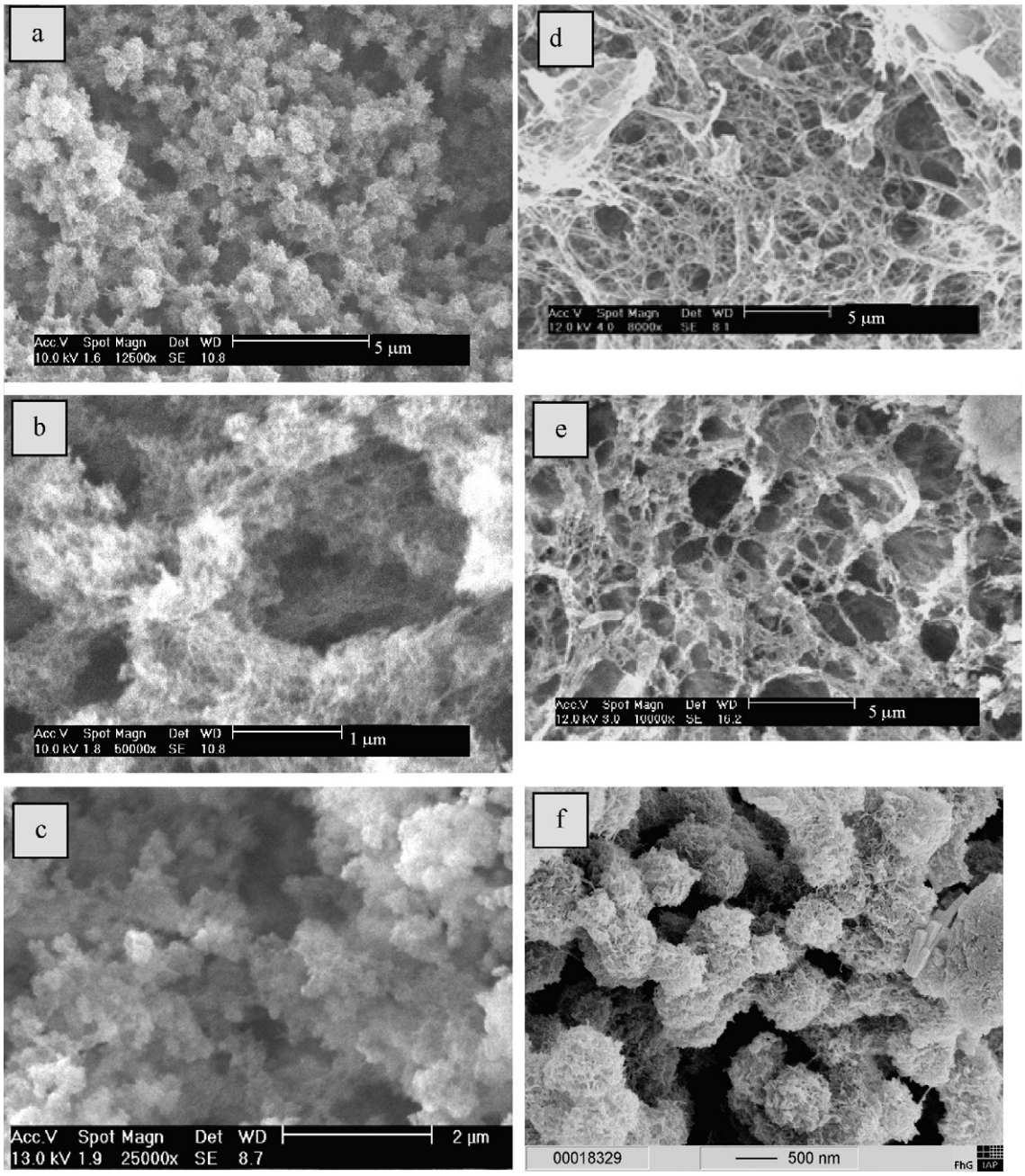


**Fig. 4.** . SEM images of aerocellulose from 3% (a and b) and 15% (c) cellulose–EMIMAc solutions, and from gelled 5% cellulose–8% NaOH–water (d, published with permission from Gavillon & Budtova, 2008, Copyright 2008 American Chemical Society), solid 3% Solucell–NMMO (e, published with permission from Gavillon & Budtova, 2008, Copyright 2008 American Chemical Society) and molten 3% Solucell–NMMO (f, published with permission from Gavillon & Budtova, 2008, Copyright 2008 American Chemical Society).

erate cellulose of a given shape. For example, it will take about 50 h to regenerate a 1 cm thick 3% cellulose disk.

### 3.2. Aerocellulose morphology, density and pore size distribution

A representative morphology of aerocellulose prepared from cellulose–EMIMAc solutions of low (3%) and high (15%) cellulose concentrations are shown in Fig. 4. The system is with the open pores of the size from few hundreds of nanometers to a few microns. Cellulose is in a form of "globules" attached to each other; their size decreases with the increase of cellulose concentration (see Fig. 4 a and c). The globules themselves are composed of "fibrous" cellulose (Fig. 4b). Similar open-pores morphology with the same pore sizes was obtained for the aerocelluloses from cellulose–NaOH–water and cellulose–NNMO solutions (Gavillon & Budtova, 2008; Sescousse & Budtova, 2009).

An interesting trend can be seen in the fine morphology of different aerocelluloses made from cellulose–ionic liquid solutions (Fig. 4a–c), from gelled cellulose–NaOH and cellulose–NMMO solutions (Fig. 4d–f, images taken from Gavillon & Budtova, 2008). The globular structure is observed for cellulose–ionic liquid solutions (Fig. 4a–c) and for aerocellulose made from molten cellulose–NMMO monohydrate solution (Fig. 4f) while a "net" of cellulose strands is seen for aerocellulose from gelled cellulose–NaOH–water and solid cellulose–NMMO monohydrate solutions (Fig. 4d and e, respectively). The reason of this difference was suggested in Gavillon and Budtova (2008) where aerocelluloses from molten cellulose–NMMO monohydrate, solid

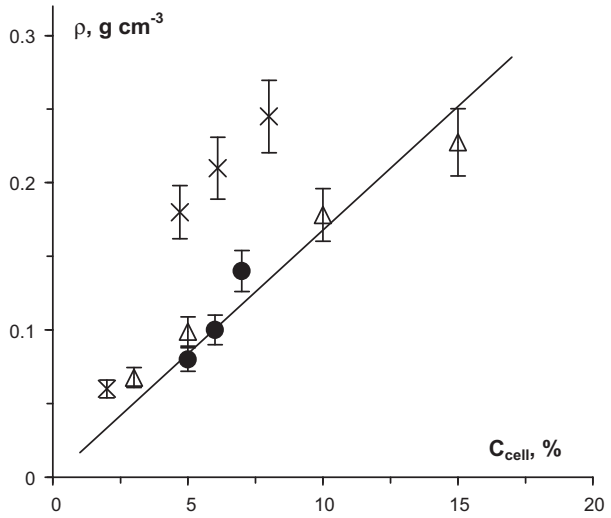


**Fig. 5.** Aerocellulose density as a function of the initial cellulose concentration in solutions of cellulose–EMIMAc (open points), cellulose–8% NaOH–water (dark points) and Solucell–NMMO (crosses). The line is linear approximation $y = 0.0168x$.

cellulose–NMMO monohydrate and gelled cellulose–NaOH–water solutions were compared. In the two latter cases the sample before regeneration is already phase separated into free solvent (crystals of NMMO monohydrate or NaOH–water hydrates) and cellulose + bound solvent. Regeneration occurs in two steps: water is first diluting regions with "free" solvent, and then removing the rest of solvent bound to cellulose. In the liquid (or molten) cellulose–NMMO monohydrate solution cellulose is spatially homogeneously distributed and phase separation occurs in one step, via spinodal decomposition (Biganska & Navard, 2009) creating regular small spheres (Fig. 4f). The morphology obtained for the aerocellulose from cellulose–EMIMAc is very similar to the one from molten cellulose–NMMO monohydrate: indeed, these systems are in the same solution state, contrary to gelled or solid (crystalline) solutions; phase separation during regeneration occurs in one step.

The density $\rho$ of aerocellulose as a function of the initial cellulose concentration is shown in Fig. 5 for EMIMAc, NaOH and NMMO routes. Data shown for cellulose–8% NaOH–water system do not include aerocellulose prepared with a foaming agent as far as it was not possible to calculate the initial cellulose concentration in the samples with air bubbles. While the data for ionic liquid and NaOH routes fall on the same linear dependence, aerocellulose from NMMO route has a slightly higher density. The most probable reason is different drying procedure parameters and thus different samples' densification: aerocelluloses from ionic liquid and NaOH were dried in Centre Energétique et Procédés, Mines ParisTech, France (the procedure is described in Section 2.2: mild conditions and slow depressurization) while aerocellulose from NMMO monohydrate solutions was dried in Natex, Austria (higher $CO_2$ temperature and quicker depressurization (Gavillon, 2007)).

One of the commonly used ways of determination of pore size distribution is mercury porosimetry. However, aerocellulose samples were completely compressed under applied pressure and no mercury entered the pores (Fig. 6). This phenomenon had already been described for some aerogels (for example, based on cellulose acetate (Fischer, Rigacci, Pirard, Berthon-Fabry, & Achard, 2006; polyurethane (Pirard et al., 2003), silica (Majling, Komarneni, & Fajnor, 1995; Scherer, Smith, Qiu, & Anderson, 1995) and silica-zirconia (Pirard, Blacher, Brouers, & Pirard, 1995)). A buckling theory for hyper-porous materials was developed by Pirard et al. (1995) allowing building pore size distribution according to the equation correlating the size of the largest pores $L$ remaining after

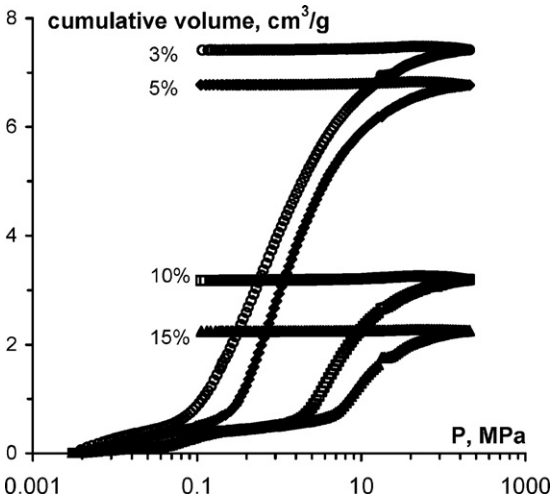


**Fig. 6.** Cumulative volume as a function of applied pressure for the aerocellulose from cellulose–EMIMAc of various initial cellulose concentrations.

compression at pressure $P$:

$$L = \frac{k}{P^{0.25}} \quad (1)$$

where $k$ is a constant depending on pore wall thickness and Young modulus and is to be determined in separate experiments from porous volume evolution during isostatic compression (Pirard et al., 2003).

The constant $k$ had never been determined for aerocelluloses and this task was not in the scope of our work. To give a general idea of the pore size distribution, arbitrary units for pore diameter were used supposing, in the first approximation, that $k$ is constant for various initial cellulose concentrations that remains to be proved. The result is shown in Fig. 7 for three initial cellulose concentrations. As expected, higher cellulose concentration, smaller are pores: the size distribution is shifted towards lower values. The results obtained with mercury porosimetry experiments will be used for the calculation of sample Young modulus; it will be compared with the mechanical properties of aerocellulose obtained from direct compression measurements in the next section.

The distribution of pore sizes in the range of mesopores was obtained using nitrogen adsorbtion–desorption method. The result of BET analysis for two representative aerocellu-

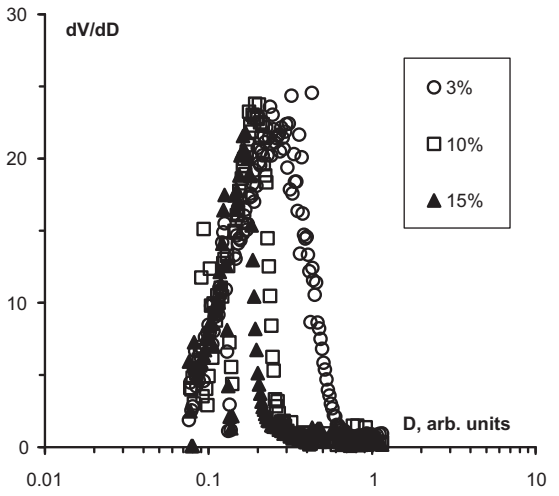


**Fig. 7.** Qualitative pore size distribution in aerocellulose from cellulose–EMIMAc solutions of 3, 10 and 15% obtained by applying Eq. (1) to mercury porosimetry data.

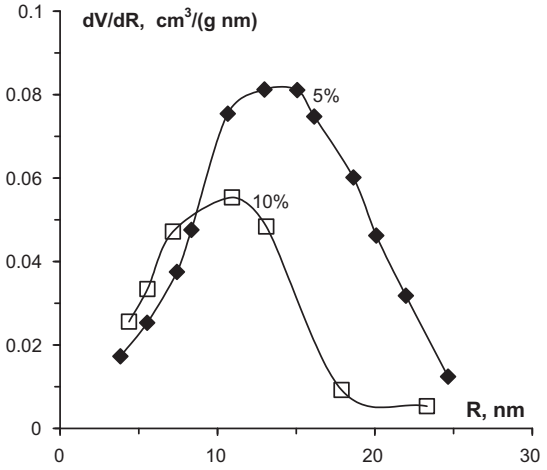


**Fig. 8.** Pore size distribution in the mesopores range for aerocellulose obtained from 5 and 10% cellulose–EMIMAc solutions. The lines are given to guide the eye.

loses from cellulose–EMIMAc is shown in Fig. 8. The radius of the pores in the nanometer range is around 10 nm; it slightly decreases with the increase of the initial cellulose concentration. The surface area varies from 230 $m^2/g$ for the aerocellulose from 3% cellulose–EMIMAc solution to 130 $m^2/g$ for 15% solution. Similar results were reported for aerocellulose made from cellulose–NMMO route (Liebner et al., 2009).

### 3.3. Mechanical properties of aerocelluloses

Stress–strain curves obtained from the uniaxial compression of aerocellulose prepared from cellulose–EMIMAc solutions are presented in Fig. 9. During compression no sample buckling was noticed, the cross-section area did not change and thus, in the first approximation, Poisson ratio can be taken equal to zero, as it was reported for some other natural foams (cork, for example). Stress–strain dependence are characterised by three regimes: (a) linear elastic region from which Young modulus $E$ can be determined; (b) a stress plateau, corresponding to progressive cell walls elastic buckling followed by their collapse when plastic yield is reached and (c) densification region, when opposing cell walls touch each other, broken fragments pack together and further deformation start to compress the wall material itself. After the end of compression experiment aerocellulose does not recover its shape, the density increases by several times. Aerocellulose thus

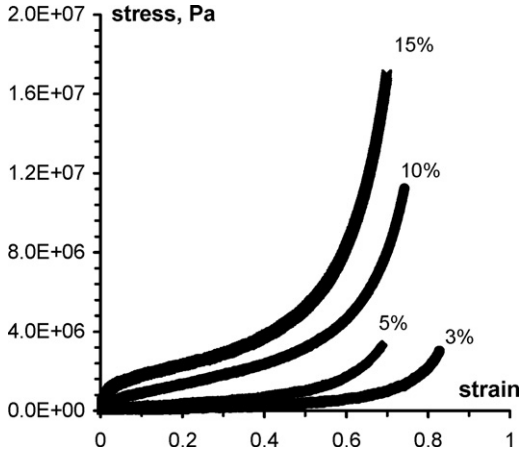


**Fig. 9.** Stress–strain data for aerocellulose from cellulose–EMIMAc solutions of various initial cellulose concentrations.

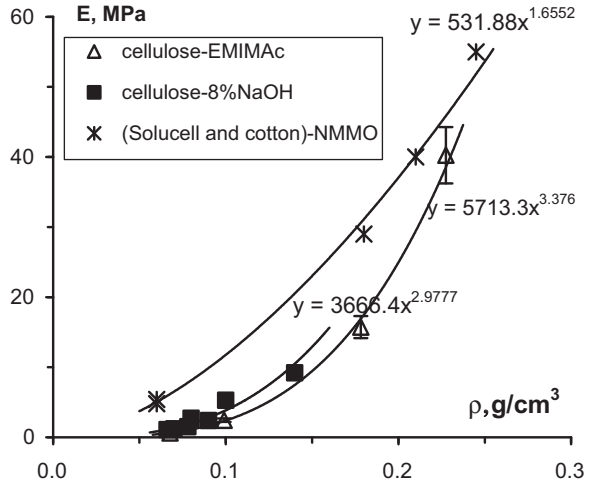


**Fig. 10.** Young modulus vs density for aerocelluloses made from low-DP cellulose (Avicel) dissolved in 8% NaOH–water and in EMIMAc and high-DP cellulose (Solucell and cotton) dissolved in NMMO. Lines are power law approximations.

behaves as an elastic–plastic foam. The linear elastic behaviour ends when the material starts to yield and reaches its compressive yield strength, $\sigma_{pl}$. The second region of the compression curve is characterised by a low slope as compared with the other two regions. This "plateau" enables porous materials to absorb large amount of energy, $W$ ($J/m^3$), without experiencing a large increase in stress. The absorption energy during the plastic deformation is defined as the area under the stress–strain curve taken up to 40% strain. The third region is characterised by a steep increase in the stress–stain curve corresponding to material densification. Each material characteristic, $E$, $\sigma_{pl}$ and $W$, will be compared for aerocelluloses obtained from different routes (ionic liquids, NaOH–water and NMMO monohydrate); they will be analysed as a function of density. In general, the increase of cellulose initial concentration (which leads to aerocellulose density increase) leads to the decrease of pore size and increase of cell wall thickness. The resistance to cell wall bending and collapse is thus increased resulting in a higher modulus and plateau stress, and the cell walls touch each other "sooner" reducing the strain at which densification begins, as demonstrated in Fig. 9.

For porous materials, foams and aerogels, a scaling relationship between material mechanical characteristics and bulk density was suggested, such as for example, $E \sim \rho^n$. The open-cell regular foam model predicts $n \approx 2$ (Gibson & Ashby, 1997); for aerogels the exponent was shown to be higher, $n \approx 2.5$–4 (see, for example $n = 2.7$ for resorcinol–formaldehyde aerogels (Pekala, Alviso, & LeMay, 1990), $n = 3.2$ and $n = 3.7$ for silica aerogels (Cross, Goswin, Gerlach, & Fricke, 1989; Woignier, Phalippou, & Vache, 1989), respectively). The reason of this difference can be found in the formation of aerogel network itself during a sol–gel transition: gel structure has a lot of defects such as dangling ends and loops which do not participate to material response to mechanical stresses. Aerocelluloses are neither aerogels that are obtained via chemical gelation nor foams that are made by introducing gas bubbles into a continuous medium. Aerocellulose structure is formed during cellulose regeneration (coagulation) from a solution into a non-solvent; many structural defects should also be created during this process and thus the scaling exponent is expected to be similar to the one found for aerogels.

Young modulus of various aerocelluloses as a function of density is shown in Fig. 10. Here the results obtained on aerocellulose from foamed gelled cellulose–8% NaOH–water route are included. The values of $E$ for the samples from the same low molecular weight microcrystalline cellulose, obtained via dissolution in 8%

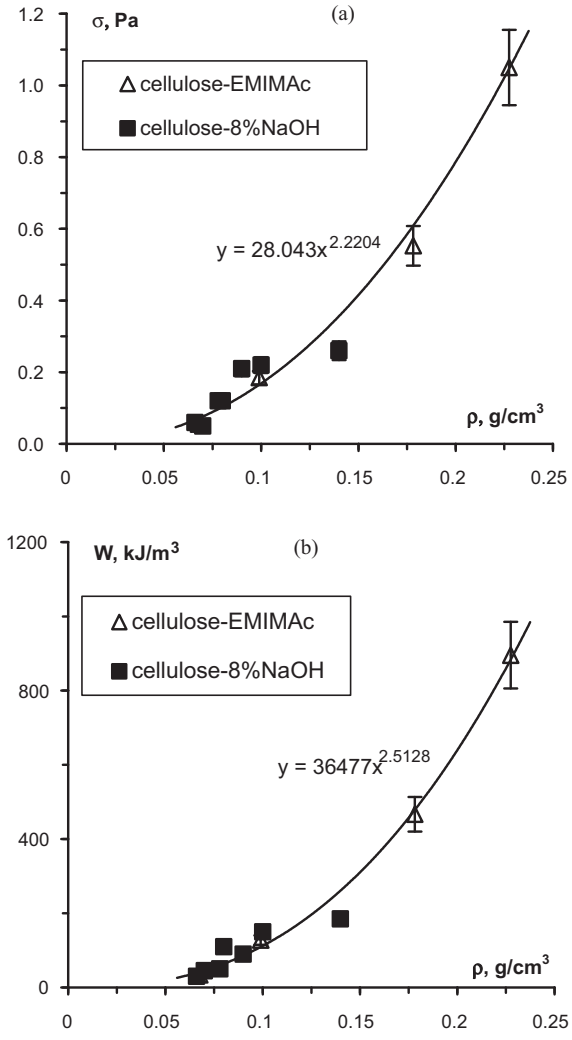


**Fig. 11.** Compressive yield strength (a) and the absorption energy (b) vs density for aerocelluloses from cellulose–EMIMAc and cellulose–8% NaOH–water routes. Lines are power law approximations.

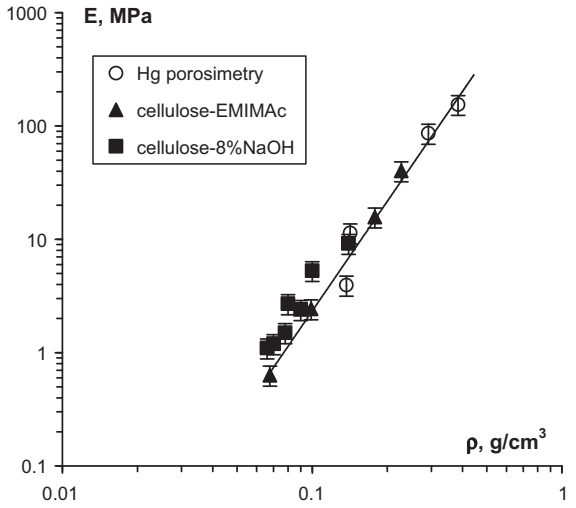


**Fig. 12.** Young modulus as a function of density for aerocelluloses made from cellulose–EMIMAc and cellulose–8% NaOH–water solutions (dark points, they are the same data as in Fig. 10) together with $E$ calculated from mercury porosimetry data (open circles) for the aerocellulose prepared from cellulose–EMIMAc solutions. Line is the power law approximation with the exponent 3.2.

NaOH or in EMIMAc, are very similar, and show the same trend vs density (Fig. 10). Their scaling exponents are $n = 3$–3.4 confirming the hypothesis that aerocelluloses are aerogel-like materials. Higher moduli values for aerocellulose from NMMO route were obtained; the most probable reason is larger cellulose molecular weight. Similar Young modulus values, of 1–10 MPa, were reported for aerocellulose from cellulose–NMMO route (Liebner et al., 2009) for samples made from various celluloses of the initial 3% solutions and final densities around 0.06 g cm$^{-3}$. Surprisingly, we found a very low scaling exponent for our aerocellulose from NMMO route, $n = 1.7$ (Fig. 10). More data on the mechanical properties of this type of aerocellulose are needed to confirm this result.

The compressive yield strength and the absorption energy as a function of aerocellulose density are presented in Fig. 11a and b, respectively. The results for both preparations routes, EMIMAc and 8% NaOH, fall on the same scaling trends: $\sigma \sim \rho^{2.2}$ and $W \sim \rho^{2.5}$. The exponents obtained are again very similar to the ones observed for aerogels (Pekala et al., 1990).

As mentioned in the previous section, the results obtained from mercury porosimetry can be used to deduce the mechanical properties of the porous material (Cross et al., 1989; Majling et al., 1995; Pirard & Pirard, 1997; Pirard et al., 1995; Scherer et al., 1995). The bulk modulus $K$ is known to be a constant correlating applied pressure $P$ and volumetric strain $\Delta V/V$: $P = K(\Delta V/V)$. $\Delta V/V$ is a product of the cumulative volume and sample (bulk) density $\rho$. Thus the bulk modulus can be calculated from the slope $\alpha$ of the early linear stage of compression dependence, pressure vs cumulative volume (inverted Fig. 6) as $K = \alpha/\rho$. Young modulus was then calculated from the known rule correlating $E$, $K$ and Poisson ratio $\nu$, the latter was taken equal to zero: $E = 3K(1 - 2\nu) = 3K$. The results are summarized in Fig. 12 where $E$ determined from porosimetry experiments on aerocellulose made from cellulose–EMIMAc is plotted together with the Young modulus obtained from compression data for the same aerocellulose. Data for the compressed aerocellulose from cellulose–8% NaOH–water route are also shown. The power law obtained for $E$ vs density from porosimetry, with the scaling exponent $n = 3.2$, shows an excellent correspondence with the scaling obtained from direct compressions measurements: for aerocellulose from cellulose–EMIMAC $n = 3.4$ and from cellulose–8% NaOH–water $n = 3$. A very similar exponent, $n = 3.3$, was obtained for aerogels based on a cross-linked cellulose acetate (Fischer et al., 2006).

## 4. Conclusions

Aerocellulose from cellulose–ionic liquid solutions was prepared via cellulose dissolution, regeneration and drying in supercritical $CO_2$ conditions. The properties of aerocellulose were compared with the ones of samples made with the same procedure but via cellulose dissolution in NMMO monohydrate and in 8% NaOH–water.

The kinetics of cellulose regeneration in water from cellulose–EMIMAc and cellulose–BMIMCl was investigated. Diffusion coefficients of EMIMAc and BMIMCl were obtained and found to weakly depend on cellulose concentration within the range of cellulose concentration studied.

The porosity of aerocellulose was studied using mercury intrusion and nitrogen adsorption methods. Samples were compressed under mercury pressure and thus only qualitative pore size distribution was deduced. Nitrogen adsorption experiments showed the presence of mesopores of the average size of 10–20 nm and specific surface area of about 150–200 m$^2$/g. The density of aerocelluloses was from 0.06 to 0.20 g/cm$^3$. The "bead-like" morphology of aerocellulose from cellulose–ionic liquid solutions was similar to the one of samples obtained from "molten" cellulose–NMMO monohy-

drate solutions. The difference with the "net-like" morphology of aerocellulose from solid cellulose–NMMO monohydrate or gelled cellulose–NaOH–water solutions was explained by different paths on a phase diagram that the system is taking during coagulation process.

The mechanical properties of aerocelluloses from EMIMAc, NMMO and 8% NaOH were measured and compared. For the samples made from cellulose of the same molecular weight and prepared in the same drying conditions Young's modulus was only controlled by density. It was found that the Young's modulus is power-law density dependent with the scaling exponent of about 3, similar to aerogels. This aerogel-like and not foam-like behaviour was explained by the presence of many defects in the overall network structure of aerocellulose formed during cellulose regeneration. Finally, a good match was found between the Young moduli obtained from mechanical compression and mercury experiments.

## Acknowledgments

This work was supported by two ANR (France) projects, "Carbocell" ANR-06-MAPR-0004 and "Nanocell" ANR-09-HABISOL-010, and the EC 6th framework, "Aerocell" project NMP3-CT2003-505888. Authors are grateful to P. Ilbizian (Centre Energétique et Procédés, Mines ParisTech, France) for performing supercritical $CO_2$ drying and to B. Simon (Saft, France) for the measurements of aerocellulose porosity.

## References

Aaltonen, O., & Jauhiainen, O. (2009). The preparation of lignocellulosic aerogels from ionic liquid solutions. *Carbohydrate Polymers*, *75*, 125–129.

Biganska, O., & Navard, P. (2005). Kinetics of precipitation of cellulose from cellulose–NMMO–water solutions. *Biomacromolecules*, *6*, 1948–1953.

Biganska, O., & Navard, P. (2009). Morphology of cellulose objects regenerated from cellulose–N-methylmorpholine N-oxide–water solutions. *Cellulose*, *16*, 179–188.

Cai, T., Zhang, H., Guo, Q., Shao, H., & Hu, X. (2010). Structure and properties of cellulose fibers from ionic liquids. *Journal of Applied Polymer Science*, *115*, 1047–1053.

Cross, J., Goswin, R., Gerlach, R., & Fricke, J. (1989). Mechanical properties of $SiO_2$-aerogels. *Revue de Physique Appliquée, Colloque C4, Supplément au n°4 avril*, *24*. C4-185–C4-190

Deng, M., Zhou, Q., Du, A., Kasteren, J. M. N., & Wang, Y. (2009). Preparation of nanoporous cellulose foams from cellulose–ionic liquid solutions. *Materials Letters*, *63*, 1851–1854.

Duchemin, B. J. C., Staiger, M. P., Ticker, N., & Newman, R. H. (2010). Aerocellulose based on all-cellulose composites. *Journal of Applied Polymer Science*, *115*, 216–221.

Egal, M., Budtova, T., & Navard, P. (2007). Structure of aqueous solutions of microcrystalline cellulose/sodium hydroxide below 0 °C and the limit of cellulose dissolution. *Biomacromolecules*, *8*, 2282–2287.

Fischer, F., Rigacci, A., Pirard, R., Berthon-Fabry, S., & Achard, P. (2006). Cellulose-based aerogels. *Polymer*, *47*, 7636–7645.

Gavillon, R. (2007). *Preparation and characterisation of ultra-porous cellulose material*. PhD thesis, CEMEF/Ecole des Mines.

Gavillon, R., & Budtova, T. (2007). Kinetics of cellulose regeneration from cellulose–NaOH–water gels and comparison with cellulose–NMMO–water solutions. *Biomacromolecules*, *8*, 424–432.

Gavillon, R., & Budtova, T. (2008). Aerocellulose: New highly porous cellulose prepared from cellulose–NaOH aqueous solutions. *Biomacromolecules*, *9*, 269–277.

Gericke, M., Schlufter, K., Liebert, T., Heinze, T., & Budtova, T. (2009). Rheological properties of cellulose/ionic liquid solutions: From dilute to concentrated states. *Biomacromolecules*, *10*, 1188–1194.

Gibson, L. J., & Ashby, M. F. (1997). *Cellular solids. Structure and properties* (2nd ed.). Cambridge University Press.

Innerlohinger, J., Weber, H. K., & Kraft, G. (2006). Aerocellulose: Aerogels and aerogel-like materials made from cellulose. *Macromolecular Symposia*, *244*, 126–130.

Jin, H., Nishiyama, T., Wada, M., & Kuga, S. (2004). Nanofibrillar cellulose aerogels. *Colloids and Surfaces A: Physicochemical Engineering Aspects*, *240*, 63–67.

Liebner, F., Haimer, E., Potthast, A., Loidl, D., Tschegg, S., Neouze, M.-A., et al. (2009). Cellulosic aerogels as ultra-lightweight materials. Part 2. Synthesis and properties. *Holzforschung*, *63*, 3–11.

Liebner, F., Haimer, E., Wendland, M., Neouze, M. A., Schlufter, K., Miethe, P., et al. (2010). Aerogels from unaltered bacterial cellulose: Application of scCO(2) drying for the preparation of shaped, ultra-lightweight cellulosic aerogels. *Macromolecular Bioscience*, *10*, 349–352.

Liebner, F., Potthast, A., Rosenau, T., Haimer, E., & Wendland, M. (2008). Cellulose aerogels: Highly porous, ultra-lightweight materials. *Holzforschung*, *62*, 129–135.

Lin, C.-X., Zhan, H.-Y., Liu, M.-H., Fu, S.-Y., & Lucia, L. A. (2009). Novel preparation and characterisation of cellulose microparticles functionalised in ionic liquids. *Langmuir*, *25*, 10116–10120.

Liu, H., Sale, K. L., Holmes, B. M., Simmons, B. A., & Singh, S. (2010). Understanding the interactions of cellulose with ionic liquids: A molecular dynamics study. *Journal of Physical Chemistry B*, *114*, 4293–4301.

Maeda, H., Nakajima, M., Hagwara, T., Sawaguchi, T., & Yano, S. (2006). Preparation and properties of bacterial cellulose aerogel. *Kobunshi Ronbunshu*, *63*, 135–137.

Majling, J., Komarneni, S., & Fajnor, V. S. (1995). Mercury porosimetry as a means to measure mechanical properties of aerogels. *Journal of Porous Materials*, *1*, 91–95.

Paakko, M., Vapaavuori, J., Silvennoinen, R., Koosen, H., Ankerfors, M., Lindstrom, T., et al. (2008). Long and entangled native cellulosel nanofibers allow flexile aerogels and hierarchically porous templates for functionalities. *Soft Matter*, *4*, 2492–2499.

Pekala, R. W., Alviso, C. T., & LeMay, J. D. (1990). Organic aerogels: Microstructural dependence of mechanical properties in compression. *Journal of Non-crystalline Solids*, *125*, 67–75.

Pirard, R., Blacher, S., Brouers, F., & Pirard, J. P. (1995). Interpretation of mercury porosimetry applied to aerogels. *Journal of Materials Research*, *10*, 2114–2119.

Pirard, R., & Pirard, J.-P. (1997). Aerogel compression theoretical analysis. *Journal of Non-Crystalline Solids*, *212*, 262–267.

Pirard, R., Rigacci, A., Marechal, J. C., Quenard, D., Chevalier, B., Achard, P., et al. (2003). Characterisation of hyperporous polyurethane-based gels by non-intrusive mercury porosimetry. *Polymer*, *44*, 4881–4887.

Quan, S.-L., Kang, S.-G., & Chin, I.-J. (2010). Characterisation of cellulose fibers electrospun using ionic liquid. *Cellulose*, *17*, 223–230.

Roy, C., Budtova, T., & Navard, P. (2003). Rheological properties and gelation of aqueous cellulose–NaOH solutions. *Biomacromolecules*, *4*, 259–264.

Scherer, G. W., Smith, D. M., Qiu, X., & Anderson, J. M. (1995). Compression of aerogels. *Journal of Non-Crystalline Solids*, *186*, 316–320.

Seki, S., Kobayashi, T., Kobayashi, Y., Takei, K., Miyashiro, H., Kikuko, H., et al. (2010). Effects of cation and anion on physical properties of room-temperature ionic liquids. *Journal of Molecular Liquids*, *152*, 9–13.

Sescousse, R., & Budtova, T. (2009). Influence of processing parameters on regeneration kinetics and morphology of porous cellulose from cellulose–NaOH–water solutions. *Cellulose*, *16*, 417–426.

Sescousse, R., Le, K. A., Ries, M. E., & Budtova, T. (2010). Viscosity of cellulose–imidazolium-based ionic liquid solutions. *Journal of Physical Chemistry B*, *114*, 7222–7228.

Swatloski, R. P., Spear, S. K., Holbrey, J. D., & Rogers, R. D. (2002). Dissolution of cellulose with ionic liquids. *Journal of the American Chemical Society*, *124*, 4974–4975.

Tsioptsias, C., Stefopoulos, A., Kokkinomalis, I., Papapdoupoulou, L., & Panayiotou, C. (2008). Development pf micro- and nano-porous composite materials by processing cellulose with ionic liquids and supercritical $CO_2$. *Green Chemistry*, *10*, 965–971.

Turner, M. B., Spear, S. K., Holbrey, J. D., & Rogers, R. D. (2004). Production of bioactive cellulose films reconstituted from ionic liquids. *Biomacromolecules*, *5*, 1379–1384.

Wendler, F., Kosan, B., Kreig, M., & Meister, F. (2009). Possibilities for the physical modification of cellulose shapes using ionic liquds. *Macromolecular Symposia*, *280*, 112–122.

Woignier, T., Phalippou, J., & Vache, R. (1989). Parameters affecting elastic properties of silica aerogels. *Journal of Materials Research*, *4*, 688–692.

Zhang, H., Wu, J., Zhang, J., & He, J. (2005). 1-Allyl-3-methylimidazolium chloride room temperature ionic liquid: A new and powerful nonderivatizing solvent for cellulose. *Macromolecules*, *38*, 8272–8277.

Zhao, Q., Yam, R. C. M., Zhang, B., Yang, Y., Cheng, X., & Li, R. K. Y. (2009). Novel all-cellulose ecocomposites prepared in ionic liquids. *Cellulose*, *16*, 217–226.